Third Order Super Twisting Based Robust Tracking of 2-DOF Helicopter with State Estimation

Ratiba Fellag [a] and Mahmoud Belhocine [b]
Industrial Automation and Robotics Division,
Centre de Développement des Technologies Avancées (CDTA), Algiers, Algeria

Abstract: This study proposes a third-order super-twisting sliding mode control algorithm combined with a Luenberger state observer for robust trajectory tracking of a two-degree-of-freedom (2-DOF) experimental helicopter. Validated on the inherently unstable and nonlinear Quanser Aero 2 platform, the method offers finite-time convergence and continuous control signals while estimating unmeasured states. The controller demonstrates accurate angular position tracking despite cross-coupling, limited measurements, uncertainties, and disturbances, effectively reducing the chattering phenomenon typically seen in conventional sliding mode control. Experimental results confirm the approach's efficacy and robustness in trajectory tracking the 2-DOF helicopter system.

1 INTRODUCTION

Unmanned Aerial Vehicles (UAVs), particularly helicopter-based systems, have experienced remarkable growth in recent years due to their adaptability and diverse applications. Helicopter-type UAVs offer unique capabilities like hovering and precise maneuvring in confined spaces. Nevertheless, controlling helicopter dynamics presents significant challenges due to the inherent nonlinearities and coupled motions, necessitating advanced control strategies to optimize their performance and exploit their full potential in various operational scenarios (Zuo et al., 2022).

Sliding mode control (SMC) is a widely used technique for managing disturbance-affected systems. It offers theoretical exact disturbance compensation by maintaining zero-valued sliding variables (Edwards & Spurgeon, 1998; Utkin, 2013). This is achieved through infinite-frequency switching. However, practical SMC implementation encounters a phenomenon known as chattering, characterized by high-frequency discontinuous oscillations, which presents a significant challenge in real-world applications (Levant, 1993).

This limitation necessitates further investigation into chattering mitigation strategies while preserving SMC's robust disturbance rejection capabilities. Higher Order Sliding Mode Control (HOSMC) has emerged as an effective strategy to eliminate chattering. HOSMC extends the principle of driving the sliding variable to zero to its higher-order derivatives. For second-order systems with a relative degree of two, representing most mechanical and electrical systems, the second-order Super-Twisting Algorithm (STA) has emerged, producing continuous control signals and avoiding chattering (Levant, 2007). Kamal et al. (Kamal & Chalanga, 2014) further generalized the STA for arbitrary relative degree systems, preserving its key characteristics while offering finite-time stabilization of both system output and its derivatives. Furthermore, it generates a continuous control signal, thereby reducing the chattering problem (Fellag et al., 2021). This approach simultaneously compensates for disturbances and uncertainties, requiring only the knowledge of the system's output and its first derivative.

In this study, we improve the control of systems with only partial state information by adding a state observer to the third-order super-twisting algorithm

[a] https://orcid.org/0000-0002-2905-3988
[b] https://orcid.org/0000-0003-3495-7444

(3-STA) based controller. The integration of a state observer addresses the practical challenge of incomplete state measurements, providing accurate estimates of the unmeasured states required for the implementation of SMC. Additionally, the state observer filters out noise and disturbances in the measurements, resulting in cleaner state estimates and improved control robustness (Luenberger, 1966). This approach not only reduces the dependency on physical sensors, thereby lowering system costs and complexity, but also extends the applicability of SMC to a wider range of systems (Chalanga et al., 2016).

The primary objective of this study is to analyze and experimentally validate the combined 3-STA controller with state estimation to stabilize the Quanser Aero2 two degrees-of-freedom (2-DOF) helicopter system under nonlinearities, cross-coupling, uncertainties, and disturbances and enable precise trajectory tracking.

2 SYSTEM DESCRIPTION AND MODELING

The Aero 2 helicopter system, shown in Figure 1, made by Quanser, consists of a base with an arm supporting two thrusters powered by DC motors. It includes high-resolution encoders, an IMU for precise control of pitch and yaw, and a data acquisition system (Quanser, 2022b). When voltage is applied to the pitch motor, the front rotor generates a force perpendicular to the body, causing torque around the yaw-axis due to aerodynamic drag. Similarly, the rear motor affects the body away from the yaw axis, mimicking the action of a tail rotor in conventional helicopters.

In order to obtain the dynamic model, Newton's second law is used for each of the helicopter axes. Friction, air resistance, and centrifugal forces are ignored to create a simplified model. This simplified model will require a robust controller to compensate for uncertainties and disturbances.

$$\begin{cases} J_p\ddot{\theta}(t) + D_p\dot{\theta}(t) + K_{sp}\theta(t) = \tau_p(t) \\ J_y\ddot{\psi}(t) + D_y\dot{\psi}(t) = \tau_y(t) \end{cases} \quad (1)$$

with: $\begin{cases} \tau_p(t) = K_{pp}D_tV_p(t) + K_{py}D_tV_y(t) \\ \tau_y(t) = K_{yp}D_tV_p(t) + K_{yy}D_tV_y(t) \end{cases} \quad (2)$

All the parameters of the dynamic model (1) and (2) are explicitly described in Table 1.

Figure 1: Quanser Aero2 helicopter system (Quanser, 2022a).

All the parameters of the dynamic model (1) and (2) are explicitly described in Table 1.

By choosing a state vector as:
$x^T(t) = \begin{bmatrix} \theta(t) & \psi(t) & \dot{\theta}(t) & \dot{\psi}(t) \end{bmatrix}^T$; $u^T(t) = \begin{bmatrix} V_p(t) & V_y(t) \end{bmatrix}^T$
the state space representation of the helicopter system is given by:

$$\begin{cases} \dot{x}_1 = x_3 \\ \dot{x}_2 = x_4 \\ \dot{x}_3 = -\dfrac{K_{sp}}{J_p}x_1 - \dfrac{D_p}{J_p}x_3 + \dfrac{D_t K_{pp}}{J_p}u_1 + \dfrac{D_t K_{py}}{J_p}u_2 \\ \dot{x}_4 = -\dfrac{D_y}{J_y}x_3 + \dfrac{D_t K_{yp}}{J_y}u_1 + \dfrac{D_t K_{yy}}{J_y}u_2 \\ y_1 = x_1 \\ y_2 = x_2 \end{cases} \quad (3)$$

Table 1: Quanser Aero2 helicopter parameters (Fellag & Belhocine, 2024a).

Symbol	Description	Value
J_p	Pitch axis inertia	0.0232 $Kg.m^2$
J_y	Yaw axis inertia	0.0238 $Kg.m^2$
D_p	Pitch axis damping	0.0020 $N.m/V$
D_y	Yaw axis damping	0.0019 $N.m/V$
K_{sp}	Pitch axis stiffness	0.0074 $N.m/V$
K_{pp}	Pitch thrust gain from front rotor	0.0032 N/V
K_{py}	Pitch thrust gain from rear rotor	0.0014 N/V
K_{yy}	Yaw thrust gain from rear rotor	0.0061 N/V
K_{yp}	Yaw thrust gain from front rotor	-0.0032 N/V
D_t	Distance btw pivot & rotor center	0.1674 m

3 CONTROLLER AND STATE OBSERVER DESIGN

This section details the design of the combined 3-STA based controller and the state observer. The control objective is to produce torques that enable precise regulation of pitch and yaw angles towards specified setpoints with minimal deviations.

3.1 State Observer Design

The full-order observer is responsible for estimating all system states, and comparing them with the physical model by analysing the error using a gain matrix (L) that multiplies the difference between the states and their estimates (Radisavljevic-Gajic, 2015). This matrix is then integrated into the theoretical model and adjusted until the error approaches zero.

Using (3), we rewrite the system state space representation as:

$$\dot{x} = Ax + Bu \qquad (4)$$
$$y = Cx + Du$$

With:

$$A = \begin{bmatrix} 0 & 0 & 1 & 0 \\ 0 & 0 & 0 & 1 \\ -K_{sp}/J_p & 0 & D_p/J_p & 0 \\ 0 & 0 & 0 & -D_y/J_y \end{bmatrix}$$

and

$$B = \begin{bmatrix} 0 & 0 \\ 0 & 0 \\ D_t K_{pp}/J_p & D_t K_{py}/J_p \\ D_t K_{yp}/J_y & D_t K_{yy}/J_y \end{bmatrix}$$

$$C = \begin{bmatrix} 1 & 0 & 0 & 0 \\ 0 & 1 & 0 & 0 \end{bmatrix} \quad \text{and} \quad D = \begin{bmatrix} 0 & 0 \\ 0 & 0 \end{bmatrix}$$

After checking the observability of our state space model (4), we design the full-order observer as follows (Fellag & Belhocine, 2024a):

$$\dot{\hat{x}}(t) = A\hat{x}(t) + Bu(t), \qquad (5)$$
$$\hat{x}(t_0) = \hat{x}_0,$$
$$\hat{y}(t) = C\hat{x}(t).$$

With $\hat{x}_0$ and t_0 initial conditions for the observer. The estimation error $e(t) = x(t) - \hat{x}(t)$ is used to construct the observation system:

$$\dot{\hat{x}}(t) = A\hat{x}(t) + Bu(t) + L(y(t) - \hat{y}(t)) \qquad (6)$$
$$= A\hat{x}(t) + Bu(t) + LCe(t),$$

where matrix L represents the observer gain matrix. From (3) and (6), we obtain the dynamics of the error as:

$$\dot{e}(t) = (A - LC)e(t), \qquad (7)$$

3.2 3-STA Controller Design

Considering the desired state vector $x_d^T = [\theta_d \quad \psi_d \quad 0 \quad 0]^T$ and initial states of the system are null.

Let e_θ and e_ψ be pitch and yaw errors defined using the estimated states and the desired states:

$$\begin{cases} \hat{e}_{1\theta}(t) = \hat{x}_1 - x_{d1} \\ \hat{e}_{2\psi}(t) = \hat{x}_2 - x_{d2} \end{cases} \qquad (8)$$

Then, their derivatives are defined by:

$$\begin{cases} \dot{\hat{e}}_{3\theta} = \hat{x}_3 - x_{d3} \\ \dot{\hat{e}}_{4\psi} = \hat{x}_4 - x_{d4} \end{cases} \qquad (9)$$

The objective is to bring these errors to zero using the 3-STA controller and the state observer.

Theorem:

For any system presented in general form:

$$\begin{cases} \dot{z}_1 = z_2 \\ \dot{z}_2 = u + f(z,t) \end{cases} \qquad (10)$$

The proposed 3-STA approach builds upon the second-order super-twisting algorithm, as presented in the work of Kamal et al. *(Kamal & Chalanga, 2014)* .

$$\begin{cases} u = -k_1 |\phi|^{1/2} \text{sign}(\phi) + P \\ \dot{P} = -k_3 \text{sign}(\phi) + d \end{cases} \qquad (11)$$

Where: $\phi = \left(z_2 + k_2 |z_1|^{2/3} \text{sign}(z_1) \right)$

and k_1, k_2, and k_3 are positive gains suitably designed, stabilizing the perturbed system in finite time. d is the perturbation satisfying $|d| \le \Delta$ ■

The detailed Lyapunov stability proof of the controller is provided in (Kamal & Chalanga, 2014).

3.2.1 Pitch Control

Assuming decoupled system, and using (3), (8), (9), and (11), the closed-loop system for pitch regulation using the 3-STA approach and state estimation is obtained as:

$$\begin{cases} \dot{x}_1 = \hat{x}_3 \\ \dot{x}_3 = -k_{1\theta} |\phi_\theta|^{1/2} \text{sign}(\phi_\theta) + x_5 + f_\theta(\hat{x}_1, \hat{x}_3) \\ \dot{x}_5 = -k_{3\theta} \text{sign}(\phi_\theta) + \zeta_\theta \end{cases} \qquad (12)$$

with:
$$\phi_\theta = \left(\hat{e}_{2\theta} + k_{2\theta} \mid \hat{e}_{1\theta} \mid^{2/3} \text{sign}(\hat{e}_{1\theta})\right) \quad \text{and}$$
$$x_5 = P_\theta + f_\theta(\hat{x}_1, \hat{x}_3)$$

If gains $k_{1\theta}$, $k_{2\theta}$ and $k_{3\theta}$ are chosen carefully and disturbance $|\zeta_\theta| \le \Delta_\theta$, then the controller in (12) stabilizes the pitch subsystem in finite time.

3.2.2 Yaw Control

Following the same methodology to design the 3-STA controller for the yaw axis, using (3), (8), (9), and (11) the closed-loop system for yaw regulation using the proposed approach is given by:

$$\begin{cases} \dot{x}_2 = \hat{x}_4 \\ \dot{x}_4 = -k_{1\psi} \mid \phi_\psi \mid^{1/2} \text{sign}(\phi_\psi) + x_6 \\ \dot{x}_6 = -k_{3\psi} \text{sign}(\phi_\psi) + \zeta_\psi \end{cases} \quad (13)$$

Where:
$$\phi_\theta = \left(\hat{e}_{2\psi} + k_{2\psi} \mid \hat{e}_{1\psi} \mid^{2/3} \text{sign}(\hat{e}_{1\psi})\right)$$
and $\quad x_6 = P_\psi + f_\psi(\hat{x}_2, \hat{x}_4)$

The proposed controller in (13) stabilizes the yaw subsystem in finite time if the disturbance ζ_ψ is bounded and gains $k_{1\psi}$, $k_{2\psi}$, and $k_{3\psi}$ are carefully designed.

The two controllers in (12) and (13), though designed for decoupled subsystems, will be implemented on the real, cross-coupled system to evaluate the robustness against cross-coupling.

4 EXPERIMENTAL RESULTS

To evaluate the proposed approach, we implemented the designed controllers using the experimental setup illustrated in Figure 2. The Quanser Aero 2 platform is equipped with a real-time control system (Fellag & Belhocine, 2024b; Quanser, 2022b), namely the QUARC Real-Time Control Software, a proprietary solution from Quanser that is integrated within Simulink from MathWorks Inc.

Initial conditions for the observer $x_0 = 0$ and the system are considered null. Square input waves are used as reference signals for pitch and yaw axes. Model parameters of the Quanser Aero 2 are given in Table 1. Some of these parameters are obtained through identification, and others from the user manual (Quanser, 2022b). The gains of the controllers and the observer are adjusted through multiple experiments and are given in Table 2. Two non-

vanishing disturbance signals are introduced to assess the robustness of the controllers (Figure 3). Moreover, the system is subject to uncertainties and cross-coupling.
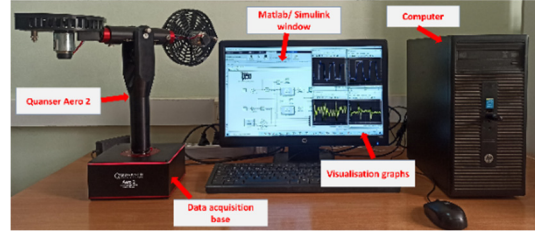

Figure 2: Experimental setup.

Table 2: Controllers gains.

Pitch controller			Yaw controller		
$k_{1\theta}$	$k_{2\theta}$	$k_{3\theta}$	$k_{1\psi}$	$k_{2\psi}$	$k_{3\psi}$
2	12	1	2	10	1

$$\begin{cases} d_\theta = 0.2 \sin(t) + 0.5 \\ d_\psi = 0.2 \sin(t) - 1 \end{cases} \quad (14)$$

The experimental results for the trajectory tracking of the pitch and yaw axes are illustrated in Figure 4 and Figure 5 respectively. The first plot shows the pitch and yaw angles over time, with the reference signals indicated by the solid lines and the system responses by the dashed lines. The second plot depicts the pitch and yaw velocities over time. The final plot shows the evolution of the third states of the closed-loop system over time.
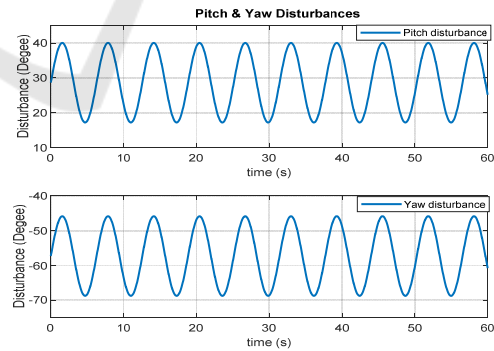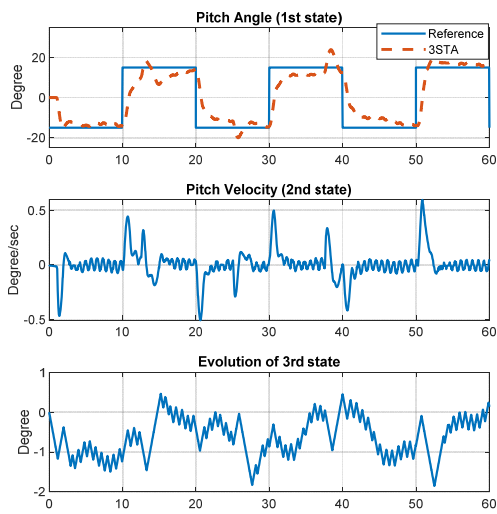

Figure 3: Pitch and yaw disturbances.

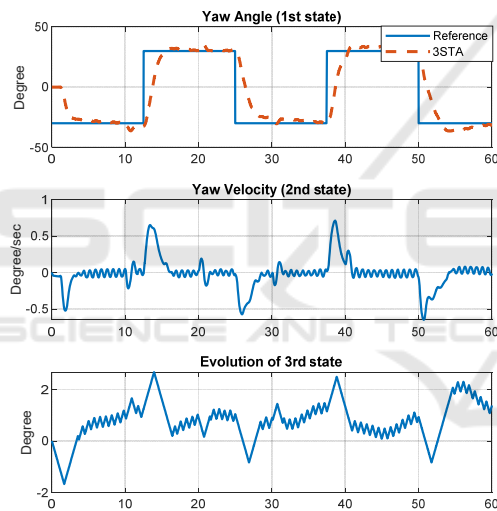Figure 4: Pitch trajectory tracking using 3-STA and state observer.

Figure 5: Yaw trajectory tracking using 3-STA and state observer.

From these figures, the 3-STA controllers combined with state observers demonstrate good tracking performance with minimal steady-state errors and robustness against disturbances, with the actual angles closely following the references for both axes. The overshoots observed in the pitch axis are caused by the yaw axis transitions, which are a direct result of the cross-coupling between the pitch and yaw axes. The pitch and yaw velocity graphs show some oscillations that are relatively small in amplitude but present throughout the experiment. This indicates that the system is experiencing dynamic responses to disturbances. Some spikes occur at step changes, indicating rapid acceleration and deceleration.

Finally, the third state curves for both pitch and yaw axes represent the added integral states (x_5 and x_6) for reconstructing and cancelling bounded disturbances. These graphs exhibit oscillatory behavior with varying amplitudes, indicating continuous adaptation to system dynamics, external disturbances, and cross-coupling effects.

Figure 6 illustrates the pitch and yaw applied motor voltages generated by the 3-STA and state estimation controllers. These signals respect the physical saturation of the motors. Although some oscillations are observed, indicating rapid adjustments in pitch and yaw voltages, the control signal is continuous as illustrated in the zoomed sections between 11s and 12s. This is due to the sinusoidal nature of applied disturbances to which the system is responding to maintain robust trajectory tracking.
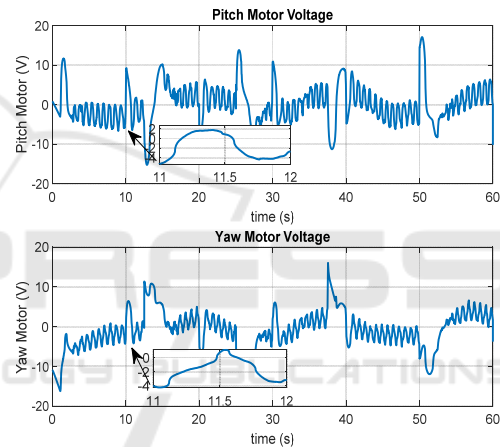

Figure 6: Pitch and yaw motor voltages.

To analyse the performance of the observer regarding pitch and yaw state estimations, Figures 7 and 8 compare measured versus estimated angular positions and velocities for pitch and yaw axes, respectively. The state observer effectively reflects the dynamics of the 2-DOF helicopter as the estimated values closely follow the measured ones. Occasional deviations are noticed in pitch and yaw angular position estimation (Figure 7), due to sensor noise, applied disturbances, or rapid changes in pitch and yaw positions. However, the state observer demonstrates a quick response to changes in both pitch and yaw, which is essential for real-time applications. Figure 8, on the other hand, indicates that the observer effectively captures the system's dynamics, with estimated pitch and yaw velocities closely following the measured values.
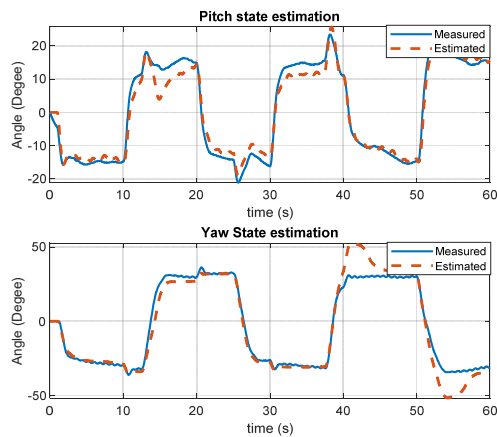
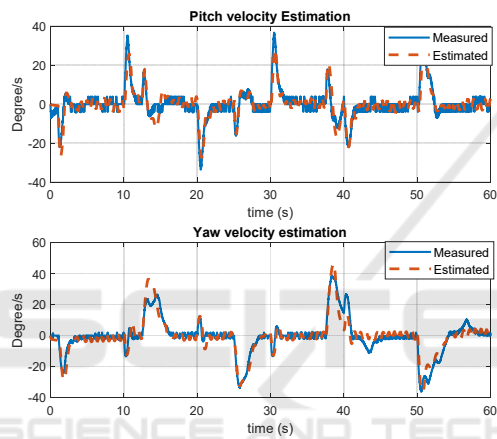Figure 7: Pitch and yaw angular position estimation.

Figure 8: Pitch and yaw velocity estimation.

5 CONCLUSION

In this study, we investigated the analysis and experimental validation of a 3-STA combined with a state observer to achieve 2-DOF helicopter trajectory tracking. The Quanser Aero 2 platform was used for real-time hardware implementation of the proposed approach. The obtained results demonstrate effective and robust trajectory tracking under cross-coupling and pitch and yaw axes continuous disturbances. The 3-STA controller relies on introducing a new state that is the integral of a discontinuous term capable of reconstructing the disturbances and cancelling them. Moreover, incorporating a state observer addresses the practical challenge of incomplete state measurements, providing accurate estimates of the unmeasured states. However, some oscillatory behaviors were noticed, suggesting further fine-tuning and the investigation of adaptive control mechanisms to further enhance the performance of the controller.

REFERENCES

Chalanga, A., Kamal, S., Fridman, L. M., Bandyopadhyay, B., & Moreno, J. A. (2016). Implementation of super-twisting control: Super-twisting and higher order sliding-mode observer-based approaches. *IEEE Transactions on Industrial Electronics*, *63*(6), 3677-3685.

Edwards, C., & Spurgeon, S. (1998). *Sliding mode control: theory and applications*. Crc Press.

Fellag, R., & Belhocine, M. (2024a). 2-DOF Helicopter Control Via State Feedback and Full/Reduced-Order Observers. 2024 2nd International Conference on Electrical Engineering and Automatic Control (ICEEAC),

Fellag, R., & Belhocine, M. (2024b). Comparative analysis of PID, fuzzy PID, and ANFIS controllers for 2-DOF helicopter trajectory tracking: simulation and hardware implementation. *Archive of Mechanical Engineering*, *vol. 71*(No 3), 323-349. https://doi.org/10.24425/ame.2024.151331

Fellag, R., Guiatni, M., Hamerlain, M., & Achour, N. (2021). Robust continuous third-order finite time sliding mode controllers for exoskeleton robot. *Archive of Mechanical Engineering*, *68*(4), 395-414.

Kamal, S., & Chalanga, A. (2014). Higher order super-twisting algorithm. 2014 13th International Workshop on Variable Structure Systems (VSS),

Levant, A. (1993). Sliding order and sliding accuracy in sliding mode control. *International journal of control*, *58*(6), 1247-1263.

Levant, A. (2007). Principles of 2-sliding mode design. *automatica*, *43*(4), 576-586.

Luenberger, D. (1966). Observers for multivariable systems. *IEEE Transactions on automatic control*, *11*(2), 190-197.

Quanser. (2022a). *Aero 2 : Reconfigurable dual-rotor aerospace experiment for controls education and research*. Retrieved 25/07/2024 from

Quanser. (2022b). *Quanser Aero 2 laboratory guide*.

Radisavljevic-Gajic, V. (2015). Full-and Reduced-Order Linear Observer Implementations in Matlab\/Simulink [Lecture Notes]. *IEEE Control Systems Magazine*, *35*(5), 91-101.

Utkin, V. I. (2013). *Sliding modes in control and optimization*. Springer Science & Business Media.

Zuo, Z., Liu, C., Han, Q.-L., & Song, J. (2022). Unmanned aerial vehicles: Control methods and future challenges. *IEEE/CAA Journal of Automatica Sinica*, *9*(4), 601-614.